THE ASTROPHYSICAL JOURNAL, 333:542–560, 1988 October 15

ROTATION CURVES FOR SPIRAL GALAXIES IN CLUSTERS. II. VARIATIONS AS A FUNCTION OF CLUSTER POSITION

BRADLEY C. WHITMORE AND DUNCAN A. FORBES
Space Telescope Science Institute

AND

VERA C. RUBIN[1]
Department of Terrestrial Magnetism, Carnegie Institution of Washington
Received 1988 February 22; accepted 1988 April 18

ABSTRACT

Rotation curves of spiral galaxies in clusters are examined using three criteria: (1) inner and outer velocity gradients; (2) residuals from synthetic rotation curves for field spirals; and (3) M/L gradients. A good correlation is found between the outer gradient of the rotation curve and the galaxy's distance from the center of the cluster, in the sense that the inner galaxies tend to have falling rotation curves, while the outer galaxies, and field galaxies, tend to have flat or rising rotation curves. A similar effect is seen in the residuals between the observed and synthetic rotation curves. A correlation is also found between the M/L gradient across a galaxy and the galaxy's position in the cluster, with the outer galaxies having steeper M/L gradients. An attempt to construct mass models produced inconclusive results. These correlations indicate that the inner cluster environment can strip away some fraction of the mass in the outer halo of a spiral galaxy or, alternatively, may not allow the halo to form.

Subject headings: galaxies: clustering — galaxies: evolution — galaxies: internal motions — galaxies: structure

I. INTRODUCTION

What role does the cluster environment play in the formation and evolution of galaxies? While a variety of possible mechanisms have been suggested for altering galaxy properties (e.g., initial conditions, ram pressure sweeping, mergers, tidal stripping), few detailed observations of galaxies in clusters are available to test different theories. However, recent observations allow us to ask at least the following two questions: "Are rotation curves for spiral galaxies in clusters different than for spiral galaxies in the field, and do any properties of the rotation curves correlate with the position of the galaxy in the cluster?"

Several recent papers have addressed the first question with contradictory results. Based on limited optical material, Rubin (1983) and Chincarini and de Souza (1985) find no qualitative differences in rotation curves of cluster and field spirals. More recently Guhathakurta *et al.* (1988) support this view with 21 cm observations. However, Burstein *et al.* (1986) report a difference in the distribution of mass types [i.e., a plot of log (V^2R) vs. log R] between field and cluster spirals.

There are a variety of properties that are known to vary with position within a cluster, including morphological types (Hubble and Humason 1931; Dressler 1980; 1984), H I content (Haynes, Giovanelli, and Chincarini 1984), and the presence of truncated and asymmetric H I disks (Warmels 1985). The present data set provides an opportunity to determine whether the distribution of mass in a galaxy is also a function of cluster position.

In Paper I of this series, Rubin, Whitmore, and Ford (1988) present the optical data and compare the range of global properties (luminosity, radius, maximum rotational velocity, and mass) between field and cluster galaxies. In the present paper we make a more quantitative analysis to determine whether a significant difference exists between the dynamical properties of cluster spirals as a function of position in the cluster. We start by comparing the inner and outer velocity gradients as defined in Whitmore (1984), progress through an examination of the residuals from the synthetic rotation curves introduced by Rubin *et al.* (1985), and finish with an examination of gradients in the mass-to-light ratio (M/L). An attempt is also made to construct detailed mass models based on luminosity profiles using a technique developed by Kent (1986). In a related paper, Forbes and Whitmore (1988) reexamine the data using the same mass type methodology used in Burstein *et al.* (1986).

II. AN EXAMINATION OF EMISSION-LINE ROTATION CURVES IN CLUSTER SPIRALS

The following two samples will be discussed in this section:

1. Hα *field sample* (*47 galaxies*).—Hα observations by Rubin *et al.* (1985) of 60 predominantly nonbarred field spirals have been trimmed to a sample of 47 by removing all galaxies located in crowded environments (i.e., local environment index of 4 or 5 from Whitmore 1984). Rotation curves from Chincarini and de Souza (1985) were not included because they did not reach to sufficient radii to perform the various types of analysis discussed below.

2. Hα *cluster sample* (*19 galaxies*).—Hα observations from Paper I of 21 galaxies in four clusters (Cancer, Hercules, Peg I, and DC 1842−63) have been trimmed to a sample of 17 by removing UGC 4375 (probable foreground galaxy), DC 12 (peculiar and emission only extends to 2″), DC 40 (face-on), and DC 47 (interacting and peculiar). Observations of NGC 4321 and NGC 4698 in the Virgo cluster by Rubin *et al.* (1985) bring the total to 19 galaxies.

[1] Visiting Astronomer, Kitt Peak National Observatory, which is operated by the Association of Universities for Research in Astronomy, Inc., under contract with the National Science Foundation.

TABLE 1

PROPERTIES OF GALAXIES IN THE Hα CLUSTER SAMPLE

Name (1)	Type (2)	M_B (mag) (3)	Distance (Mpc) (4)	R_{25} (kpc) (5)	R_f/R_{25} (6)	$R_{cluster}$ (Mpc) (7)	IG (%) (8)	OG (%) (9)	EG (%) (10)	$\Delta V_{OBS-SYN}$ (km s^{-1}) (11)	V_{SLOPE} (12)	M/L(0.8/0.1) (13)	M/L(0.8/0.4) (14)	H I Deficiency (15)
Cancer cluster:														
NGC 2558	Sab	−21.83	91.1	23.4	0.77	0.99	76	4	..	13	−34	5.1	1.3	−0.18
UGC 4329	Sc	−21.19	91.1	23.2	1.29	0.58	72	−12	11	−42	−105	1.7	0.9	0.10
UGC 4386	Sb	−22.31	91.1	25.9	0.69	1.29	59	37	...	−48	106	7.3	2.0	0.16
Virgo cluster:														
NGC 4321	Sbc	−21.53	20.0	20.1	0.73	1.38	70	14	...	7	10	4.0	1.6	0.52
NGC 4698	Sab	−20.60	20.0	11.9	0.97	2.03	...	32	...	20	137	9.1	2.3	...
Hercules cluster:														
NGC 6045	Scd	−23.40	223.0	36.1	0.83	0.25	85	−11	...	30	−121	2.0	0.8	0.25
NGC 6054	SBc	−21.49	223.0	26.4	0.98	0.25	96	−4	...	−22	−127	1.4	1.2	...
Peg 1 cluster:														
NGC 7591	SBb	−21.66	81.2	23.9	1.42	2.43	...	2	−11	−27	−24	...[a]	...[a]	−0.30
NGC 7608	Sb	−20.65	81.2	17.4	0.57	0.56	40	...	...	...	...	...	...	0.34
NGC 7631	Sb	−21.62	81.2	20.6	1.26	0.30	56	0	8	−40	−5	2.2	1.1	0.31
UGC 12417	Sc	−20.50	81.2	13.1	1.07	4.35	42	22	...	−12	37	3.9	1.9	−0.14
UGC 12498	Sb	−20.51	81.2	17.5	0.69	0.50	64	−2	...	−34	18	3.5	1.1	0.36
DC 1842−63 cluster:														
DC 2	Sb	−20.73	87.1	16.8	0.49	0.68	72	...	...	...	...	...	...	...
DC 8	Sa	−20.99	87.1	16.2	0.62	0.24	93	−18	...	...	...	1.0	0.8	...
DC 10	Sc(pec)	−19.58	87.1	9.9	0.61	0.17	41	...	...	...	...	...	...	...
DC 24	SBc	−20.16	87.1	12.8	0.78	0.23	72	−26	...	−5	−77	1.5	0.6	...
DC 39	SBc	−21.20	87.1	17.1	1.29	0.28	...	0	−5	−63	18	...[a]	1.3	...
WR 42	Sa	−20.94	87.1	18.3	0.66	1.33	51	30	...	−27	93	3.9	1.7	...
WR 66	SBb	−20.77	87.1	24.1	1.10	1.52	74	1	...	−9	−31	5.0	1.3	...

NOTES.—Key to columns is as follows:

Col. (2).—Hubble Type from Sandage and Tammann 1981.

Col. (3).—Absolute B magnitude from RC2 and corrections for internal and galactic extinction using the same equations as Paper I.

Col. (4).—Distance from heliocentric velocity corrected to the Local Group using 300 sin l cos b and using $H_0 = 50$ km s^{-1} Mpc^{-1}.

Col. (5).—Radius at the 25 mag arcsec^{-2} isophote in B, corrected for internal and galactic extinction using the same equations as Paper I.

Col. (6).—Ratio of the last point measured in the rotation curve, R_f, to R_{25}.

Col. (7).—Projected distance from the center of the cluster assuming the centers are at: NGC 2563 for the Cancer cluster; NGC 4486 (M87) for the Virgo cluster; halfway between NGC 6045 and NGC 6054 in the Hercules cluster; halfway between NGC 7619 and NGC 7626 for the Peg I cluster; and at DC 19 in the DC 1842−63 cluster.

Col. (8).—Inner gradient of the rotation curve, defined as the percentage of maximum rotational velocity reached by $0.15R_{25}$.

Col. (9).—Outer gradient of the rotation curve, defined as the percentage increase of the rotation curve between $0.4R_{25}$ and $0.8R_{25}$, normalized to the maximum rotational velocity.

Col. (10).—Extended gradient of the rotation curve, defined as the percentage increase of the rotation curve between $0.8R_{25}$ and $1.2R_{25}$, normalized to the maximum rotational velocity.

Col. (11).—The difference at $0.5R_{25}$ between the observed rotation curve and a synthetic rotation curve (Rubin *et al.* 1985) using least-squares fits between $0.2R_{25}$ and $0.8R_{25}$.

Col. (12).—The slope of the residuals between the observed and synthetic rotation curves using least-squares fits between $0.2R_{25}$ and $0.8R_{25}$.

Col. (13).—Value of M/L (i.e. V^2R/L_{red}) at $0.1R_{25}$ divided by the value of M/L at $0.8R_{25}$. In cases where the rotation curve did not extend to $0.8R_{25}$, an extrapolation from $0.4R_{25}$ to the last observed point was used, with the stipulation that the observations must extend to at least $0.6R_{25}$. The only exception was for DC 8, where the value at the last observed point was used instead of the extrapolated value.

Col. (14).—Value of M/L at $0.4R_{25}$ divided by the value of M/L at $0.8R_{25}$, using the same procedure as described for col. (13).

Col. (15).—H I deficiency from Giovanelli and Haynes 1985. The higher values are for more deficient galaxies.

[a] An estimate of the M/L gradient was not made because rapid change in the rotational velocity suggests that noncircular velocities may be present.

a) Velocity Gradients

The first method used to examine rotation curves is a simple comparison of velocity gradients, as defined by Whitmore (1984) for the Hα field sample. The inner gradient (IG) is defined as the percentage of the maximum rotational velocity reached by $0.15R_{25}$, where R_{25} is the radius at the 25th B mag arcsec^{-2} isophote. The outer gradient (OG) is the percentage increase of the rotation curve between $0.4R_{25}$ and $0.8R_{25}$, normalized to the maximum rotational velocity. Because some H I rotation curves extend farther than the Hα curves, we have introduced a new parameter called the extended gradient (EG). This is defined as the percentage increase between $0.8R_{25}$ and $1.2R_{25}$, again normalized to the maximum rotational velocity. Values of IG and OG for the Hα field sample are taken from Whitmore (1984). Values of OG and IG for the Hα cluster sample are listed in Table 1. This table also includes Hubble type, absolute magnitude, distance, radius, and distance from the center of the cluster ($R_{\rm cluster}$). The central positions used to determine $R_{\rm cluster}$ are included in the notes to Table 1. They are usually coincident with the dominant central galaxy in the cluster (e.g., M87 in the Virgo cluster) or halfway between the two dominant central galaxies (e.g., NGC 7619 and NGC 7626 in the Peg I cluster). A Hubble constant of 50 km s^{-1} Mpc^{-1} is used throughout.

Figure 1 shows a plot of the outer gradient (OG) as a function of $R_{\rm cluster}$ for the Hα cluster sample. A correlation between these two properties exists (OG = 10.3 + 43.2 [±10.9] log $R_{\rm cluster}$), with a correlation coefficient of 0.73, and a probability of 99.9% that OG and $R_{\rm cluster}$ are correlated. The slope is the mean of the value of the least-squares fits of Y upon log X, and log X upon Y; the uncertainty is the 1 σ value. The average value of OG for the Hα field sample is also indicated with error bars showing the 1 σ scatter of the distribution. *This is the principal result of our paper; the rotation curves for galaxies near the centers of clusters tend to have falling rotation curves in their outer regions, while galaxies farther from the cluster center, or in the field, tend to have flat or rising rotation curves.* The most straightforward explanation is that the inner cluster environment has stripped away some fraction of the mass in the outer halo of a spiral galaxy, or alternatively, never allowed the halo to form. The strength of the correlation is especially surprising when one considers that a galaxy which appears to be near the center of a cluster may actually be an outer galaxy superposed on the central region. The strong correlation suggests that all of the galaxies with low values of $R_{\rm cluster}$ are probably located near the cluster center.

Many of the galaxies we observed near the cluster centers are Sc galaxies. For field galaxies, OG is a function of luminosity and Hubble type; lower luminosity and later type spirals generally have positive outer gradients. However, in the cluster sample even the seven galaxies with types later than Sb show the trend between OG and cluster position, with several of the Sc galaxies having negative outer gradients. This result suggests that the local environment in clusters is more influential than the galaxy type or luminosity in determining the overall dynamical parameters. The barred spirals in the sample are distributed at both small and large $R_{\rm cluster}$, and follow the same general trend.

The range of values and the mean of OG for the field sample

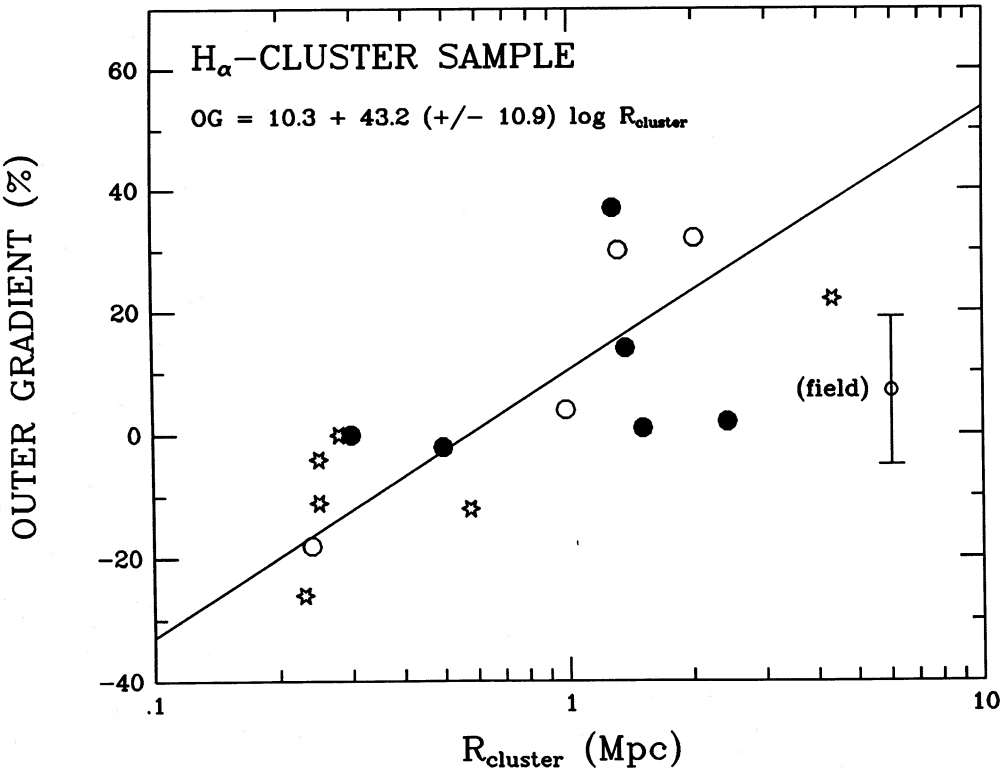

FIG. 1.—Outer gradient of the rotation curve (percentage increase from $0.4R_{25}$ to $0.8R_{25}$, normalized to $V_{\rm max}$) vs. the projected distance from the center of the cluster for the Hα cluster galaxies. Open circles are Sa galaxies; filled circles are Sb galaxies; open stars are Sc galaxies. The average value for the Hα field sample is included with error bars showing the 1 σ scatter of the distribution. Galaxies near the centers of the clusters have falling rotation curves.

are close to those for the cluster galaxies. However, while six of the 16 cluster galaxies have negative values of OG, all near the clusters' centers, only seven of the 42 field spirals have negative values of OG. We conclude that while many cluster spirals resemble field spirals, there is an additional population of galaxies near the centers of clusters whose dynamics are unlike field galaxies.

In contrast to the outer gradient, the inner gradient (IG) does not correlate with the position in the cluster. Figure 2 plots IG versus $R_{\rm cluster}$. The bar on the right shows the average value and the 1 σ scatter of the distribution for the Hα field sample. The mean value of IG for the cluster sample is slightly lower than the field sample. This may be caused by a difference in distance (i.e., resolution), Hubble type, absolute magnitude, or some combination of the three. However, when we trim the two samples to make them as similar as possible in their distributions of these three properties, the small difference between the means of IG for the cluster and field samples remain. Although there is little correlation between IG and $R_{\rm cluster}$, the galaxies near the centers of clusters do have the highest values of IG. The fact that the inner galaxies tend to be Sc galaxies, which generally have shallower inner gradients, suggests that this trend may actually be stronger than indicated by Figure 2.

b) Comparison with Synthetic Rotation Curves

One weakness of the gradient analysis is that only a small portion of the available data is actually used. Another problem is that rotation curves change as a function of Hubble type and luminosity, so a proper treatment needs to take these parameters into account. In this section we use the entire rotation curve by comparing our observations with the synthetic rotation curves defined by Rubin *et al.* (1985) for the sample of field galaxies. The synthetic curves were derived from the data from all 60 galaxies, including the 13 which we have deleted from our Hα field sample because they appear in relatively dense environments. However, this is a minor effect and will make any difference between the cluster and field samples a conservative lower limit.

The comparison is made by first constructing a synthetic rotation curve for each cluster galaxy based on Rubin *et al.* (1985; Table 6). This is done by interpolating the grid of synthetic curves for various Hubble types and absolute B magnitude to match those of the cluster galaxies. The resulting synthetic rotation curves are shown in Figure 3 of Paper I. A qualitative comparison between the observed and synthetic rotation curves for the Hα field sample shows two effects. First, in a majority of the cases the observed values at $0.5R_{25}$ fall below the synthetic rotation curves, as discussed in Paper I. Second, the galaxies with the outer rotation curves that are clearly falling relative to the synthetic curves tend to be the inner galaxies (e.g., NGC 6045 at 0.25 Mpc; NGC 6054 at 0.25 Mpc; UGC 4329 at 0.58 Mpc; DC 8 at 0.24 Mpc; and DC 24 at 0.23 Mpc) and the galaxies with the rotation curves that are clearly rising faster than the synthetic curves tend to be the outer galaxies (e.g., UGC 4386 at 1.29 Mpc; UGC 12417 at 4.35 Mpc; and WR 42 at 1.33 Mpc).

The residuals from these synthetic curves as a function of R/R_{25} are shown in Figure 3. Figure 3*a* includes the galaxies in the cluster sample within 0.8 Mpc of the cluster center; Figure 3*b* includes the cluster galaxies beyond 0.8 Mpc. A least-squares fit to the data between $0.2R_{25}$ and $0.8R_{25}$ for each individual galaxy was made. Each fit was then normalized to 0 at $0.5R_{25}$. The scatter inside $0.2R_{25}$ shows the large difference which exist in the central concentration of mass for galaxies of the same Hubble type and absolute magnitude. Most of this effect can probably be attributed to the fact that velocities in the outer region are controlled by the total mass within this radius which will dominate any irregularities in the local mass distribution. On the other hand, the same magnitude irregu-

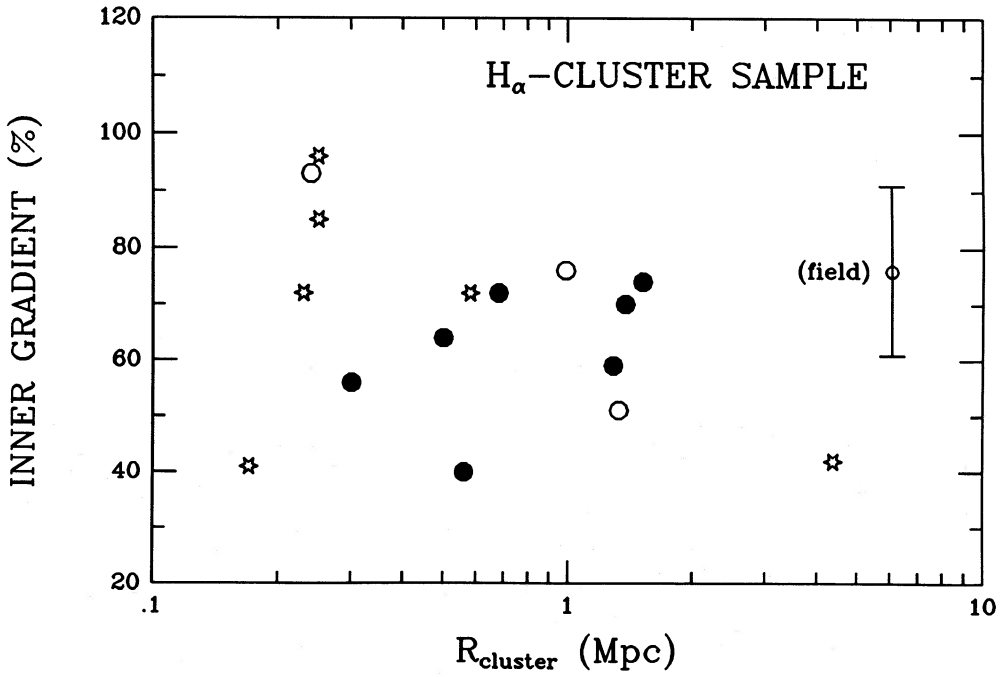

FIG. 2.—Inner gradient of the rotation curve (percentage of $V_{\rm max}$ reached by $0.15R_{25}$) vs. the projected distance from the center of the cluster for the Hα cluster galaxies. Same symbol definitions as Fig. 1.

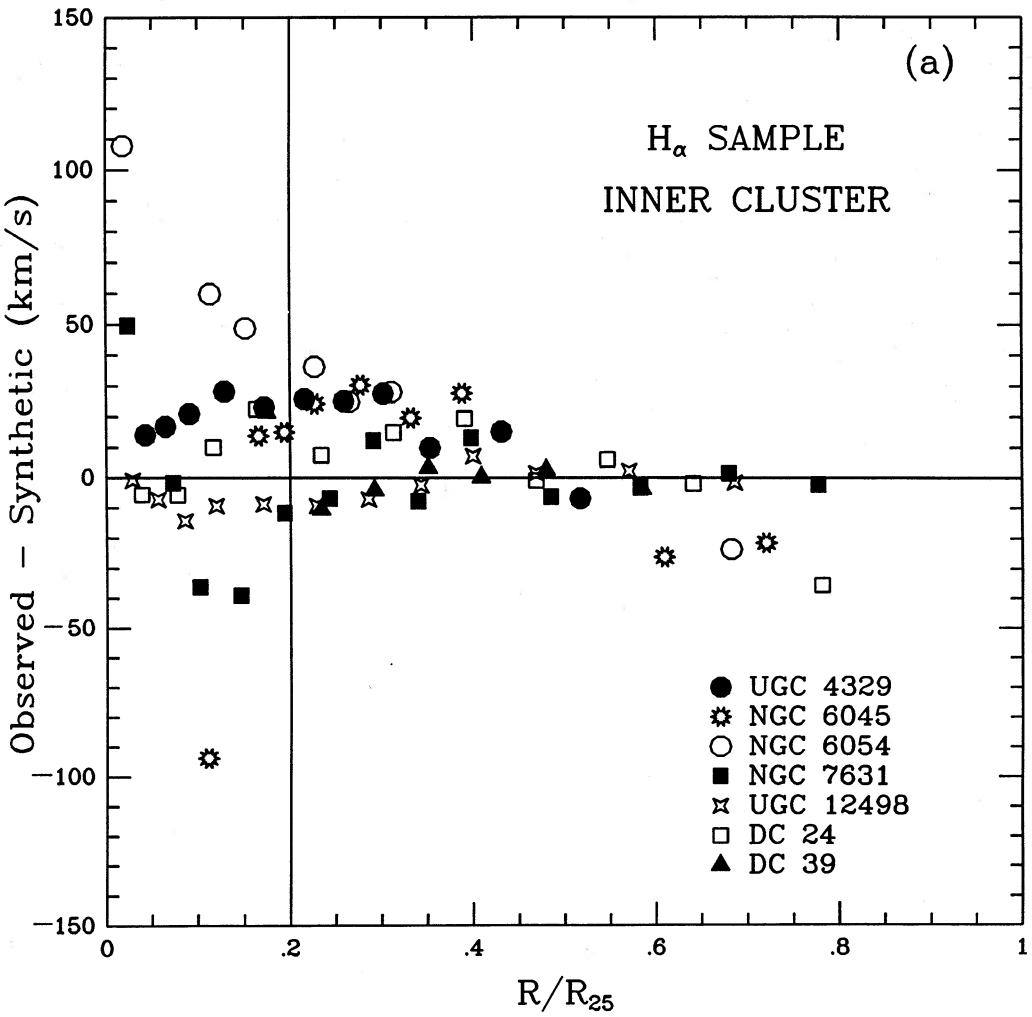

FIG. 3.—Residuals between the observed rotation curves and the synthetic rotation curve from Fig. 3 of Paper I as a function of radius. (*a*) Galaxies within 0.8 Mpc of the cluster center; (*b*) galaxies more than 0.8 Mpc from the cluster center. Beyond $0.2R_{25}$ the inner cluster galaxies have more negative slopes than the outer cluster galaxies.

larity in the inner part of a galaxy (e.g., a bar or lens) will be a much larger fraction of the total mass within that radius, so the effect on the rotation curve will be much larger. The residuals for the inner cluster sample show primarily negative values at large R/R_{25}; the residuals for the outer cluster sample show a primarily positive values at large R/R_{25}. This comparison confirms the result from the OG analysis; the rotation curves for the inner cluster galaxies are falling relative to the galaxies in the outer cluster, or to galaxies in the field.

Table 1 lists the difference between the least-squares fit and the value for the synthetic rotation curve at $0.5R_{25}$ ($\Delta V_{\rm OBS-SYN}$), and the slope of the fit ($V_{\rm SLOPE}$). Only the region between $0.2R_{25}$ and $0.8R_{25}$ has been used, with the stipulation that the data must extend to at least $0.6R_{25}$. Figure 4 shows the correlation between $V_{\rm SLOPE}$ and $R_{\rm cluster}$. This is yet another representation of the discovery that galaxies near the cluster centers have rotation curves which are different than the galaxies in the outer regions of the clusters, or in the field, in the sense that they have negative gradients with respect to the synthetic rotation curves. Inner galaxies have lower velocities at $0.5R_{25}$ than expected, since $\Delta V_{\rm OBS-SYN}$ tend to be negative ($\langle \Delta V_{\rm OBS-SYN} \rangle = -17 \pm 7$ km s^{-1}). This difference in the maximum rotational velocities for cluster and field galaxies is discussed in Paper I.

c) *M/L Gradients*

In the previous two sections we found that the rotation curves are generally falling for spiral galaxies in the central region of clusters, while rotation curves are generally flat or rising for galaxies in the outer regions of the cluster. Has the dark halo been stripped, either by tidal interactions with other galaxies or with the overall gravitational field of the cluster? Perhaps the inner cluster environment never allowed the galaxy to form a halo. Another possibility is that the inner cluster environment has modified the luminosity distribution, so that the decline in the rotation curves can be explained entirely in terms of the loss of luminous material without having to postulate a difference in the distribution of dark matter.

To address these questions we have calculated integral mass-to-light ($M/L = V^2R/L_{\rm red}$) gradients for the cluster galaxies for which we have reliable photometry. The luminosity profiles for the Hα cluster sample are from Bell and Whitmore (1988) or,

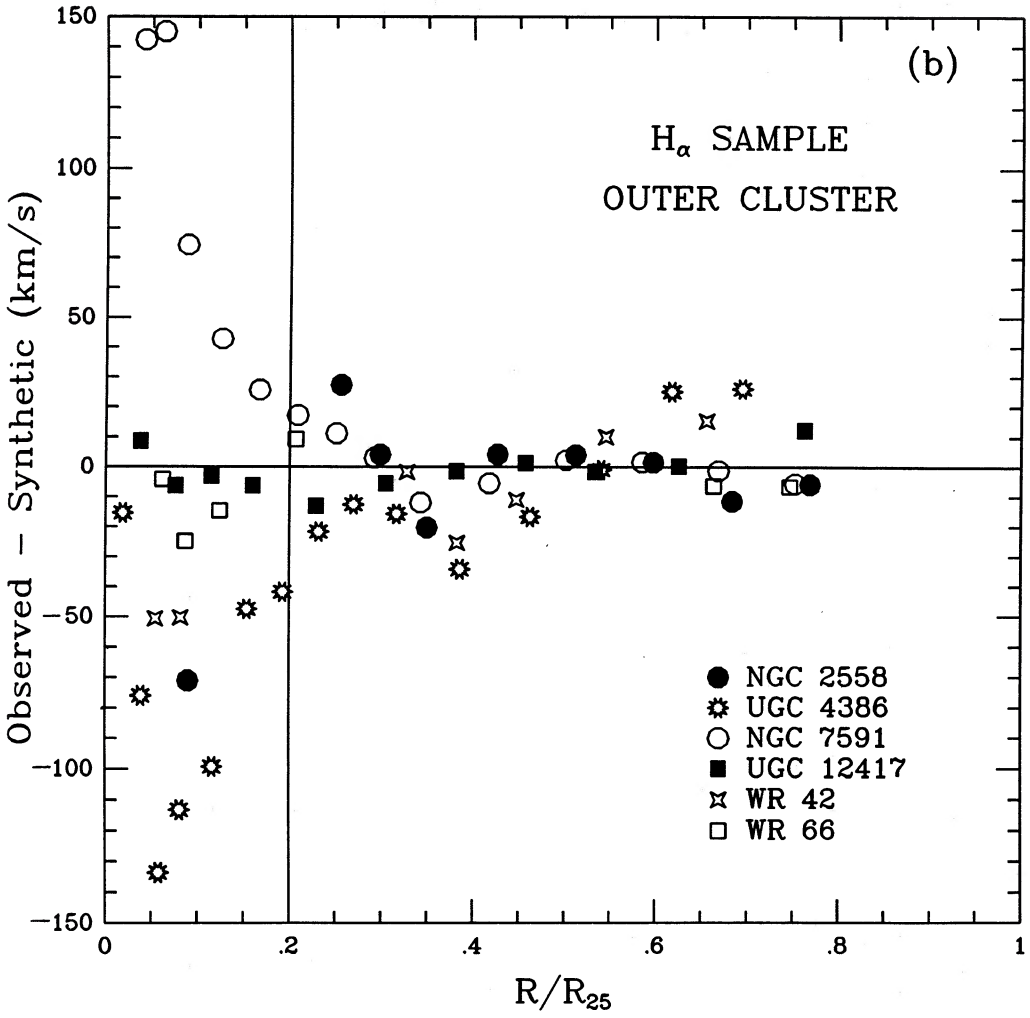

FIG. 3*b*

for the Cancer and Hercules clusters, have been obtained as part of this study (see Appendix). The total luminosity within a given radius is determined using the major axis profile and the observed ellipticity at R_{25}.

Figure 5 shows M/L as a function of the distance from the centers of the galaxies. The values of M/L have been normalized to 1.0 at $0.5R_{\rm cluster}$. The galaxies are arranged in order of the distance from the centers of the clusters. We find that the inner cluster galaxies have flatter M/L gradients than the galaxies in the outer regions of the cluster. All of the galaxies, except the few closest to the cluster centers, have integral M/L values which increase with galaxy radius. A luminous disk of constant M/L (i.e., a horizontal line in Fig. 5) is not an acceptable mass model for these galaxies.

Table 1 lists the M/L gradients from $0.1R_{25}$ to $0.8R_{25}$, and from $0.4R_{25}$ to $0.8R_{25}$, both normalized to the value of M/L at $0.8R_{25}$. The two M/L gradients are plotted versus $R_{\rm cluster}$ in Figure 6. Both parameters show strong correlations with the position in the cluster (e.g. $\log M/L[0.8/0.1] = 0.58 + 0.69$ $[\pm 0.14]$ $\log R_{\rm cluster}$), with a correlation coefficient of 0.81, and a probability of 99.9% that the two parameters are correlated. *If a strong gradient in M/L is indicative of a large fraction of dark matter in the outer regions of a galaxy, then the present sample provides evidence that the galaxies near the centers of clusters have a lower fraction of their mass in the form of dark matter than the galaxies in the outer regions of a cluster.* This is entirely consistent with our earlier result that the outer gradient of the rotation curve is negative for the galaxies near the centers of clusters, suggesting that a sizable halo does not exist for these inner galaxies.

Is the correlation between $M/L(0.8/0.4)$ and $R_{\rm cluster}$ simply a reflection of the trend between OG and $R_{\rm cluster}$, since the same measurements of the velocity are used for determining both $M/L(0.8/0.4)$ and OG? This does not appear to be the case. The inclusion of an independent parameter, the luminosity profile, should degrade the correlation by including an additional variable in the determination of M/L. However, the correlation between $M/L(0.8/0.4)$ and $R_{\rm cluster}$ is actually better than the correlation between OG and $R_{\rm cluster}$. Perhaps more convincing is the fact that IG, determined at nearly the same radius as used to determine $M/L(0.8/0.1)$, shows little correlation with $R_{\rm cluster}$ (Fig. 2), while the $M/L(0.8/0.1)$ versus $R_{\rm cluster}$ correlation is very good.

d) Mass Models

Several recent studies have used the observed luminosity distribution in spiral galaxies to construct mass models (Kalnajs 1983; Kent 1986, 1987; Anthanassoula, Bosma, and

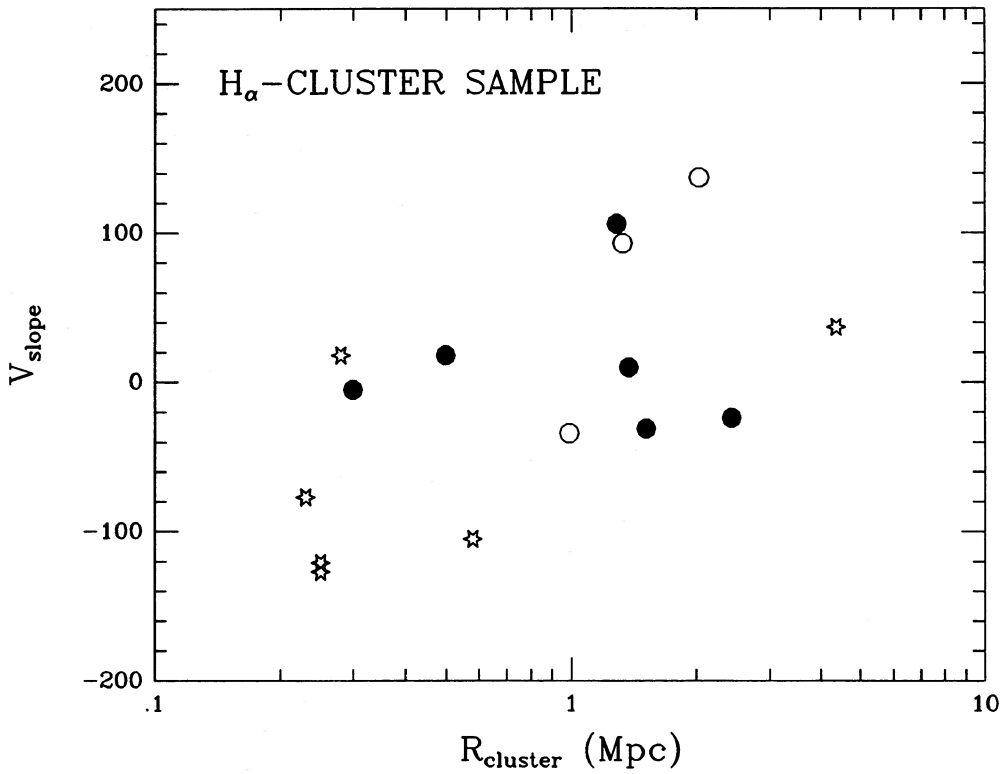

FIG. 4.—V_{slope} vs. the projected distance from the center of the cluster for the Hα cluster sample. Same symbol definition as Fig. 1. Rotation curves for the inner galaxies have shallower gradients, relative to the synthetic rotation curves, than the galaxies in the outer regions of the clusters.

Papaioannou 1987). This is an improvement over earlier models which assumed that the disk exactly follows an exponential profile. We have constructed similar mass models of the galaxies for which we have reliable photometry. A slight modification of Kent's (1986) program has been employed, with the bulge component being determined from an iterative decomposition of the luminosity profile (see Bell and Whitmore 1988 for details).

The models have a bulge and a disk component. The disk is derived from the major axis luminosity profile assuming it is circular and infinitely thin. Both the disk and bulge are assumed to have constant, but independent, value of mass-to-light ratio [M/L(bulge) and M/L(disk)]. We have chosen not to model the dark halo since it is difficult to estimate the maximum amount of dark matter that could be present in the galaxy, and even more difficult to determine the shape of the rotation curve for the halo. For example, in principle it would be acceptable to set the M/L for the bulge and disk to zero and have the observed rotation curve completely dominated by the halo. The normal procedure is to attempt to estimate the minimum amount of dark matter by fitting a "maximum disk" determined from the luminous material. If the fit with the observed rotation curve is reasonably good using the maximum disk solution, then the usual conclusion is that the luminous matter must dominate the distribution of mass. Our attempts to construct reasonable mass models for the cluster galaxies has convinced us that this procedure may *artificially* produce reasonably good fits to the data, and can therefore not be taken as evidence for small fractions of dark matter.

Although the ability to use different values for the mass-to-light ratio (M/L) of the bulge and disk is reasonable in principle, in practice it can lead to some severe problems. The value of M/L(bulge) can be adjusted to fit the inner region while the value of M/L(disk) can be used to fit the outer regions of the rotation curve. While about half our cluster galaxies could be fit with reasonable values of M/L(bulge) and M/L(disk), the other half resulted in unphysical results [e.g. negative values of M/L(bulge)]. No trend was found between the galaxies which could be adequately fit, and $R_{cluster}$. The poor quality of many of the fits caused us to abandon our attempts to produce viable mass models for the cluster galaxies using the standard procedures.

Several of Kent's (1986, 1987) models also show large differences between the M/L(bulge) and M/L(disk). Some values of M/L(bulge) are actually negative [e.g., in NGC 3054 a negative M/L(bulge) is used to lower the predicted rotation curve in the inner region to fit the observations]. The problem appears to be even more serious for the Sa galaxies, since Kent (1988) finds that half of the Sa galaxies he studied can only be fitted with M/L(bulge) = 0. Perhaps a better way to constrain future models would be to fix M/L(bulge) and M/L(disk) to the same value. Another possibility would be to use information about the photometric color, or spectral content, to fix the ratio between M/L(bulge) and M/L(disk).

e) Comparison Using Neutral Hydrogen Rotation Curves

Rotation curves determined using neutral hydrogen observations often extend well beyond the optical image of a galaxy, and may therefore provide a better diagnostic for examining the effect of the cluster environment on spiral galaxy dynamics. However, the limited spatial resolution of the H I observations, and the fact that the inner cluster galaxies may be deficient in H I, limits the usefulness of the H I observations.

We have used the same methods of analysis described in the

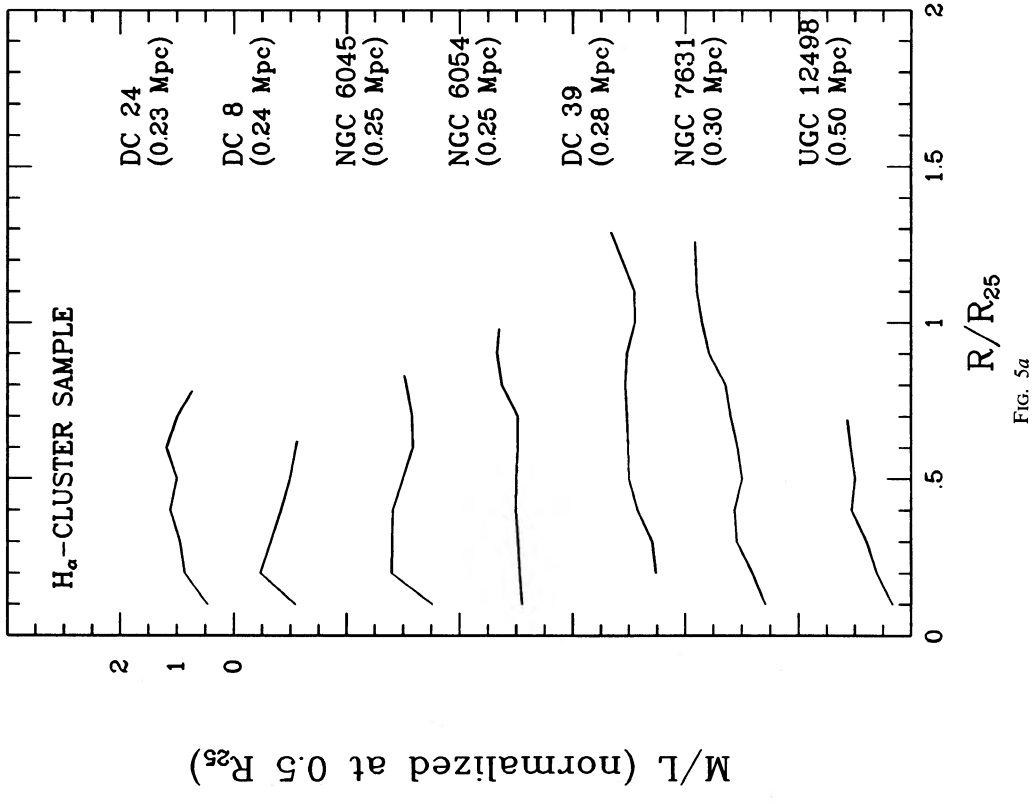

FIG. 5a

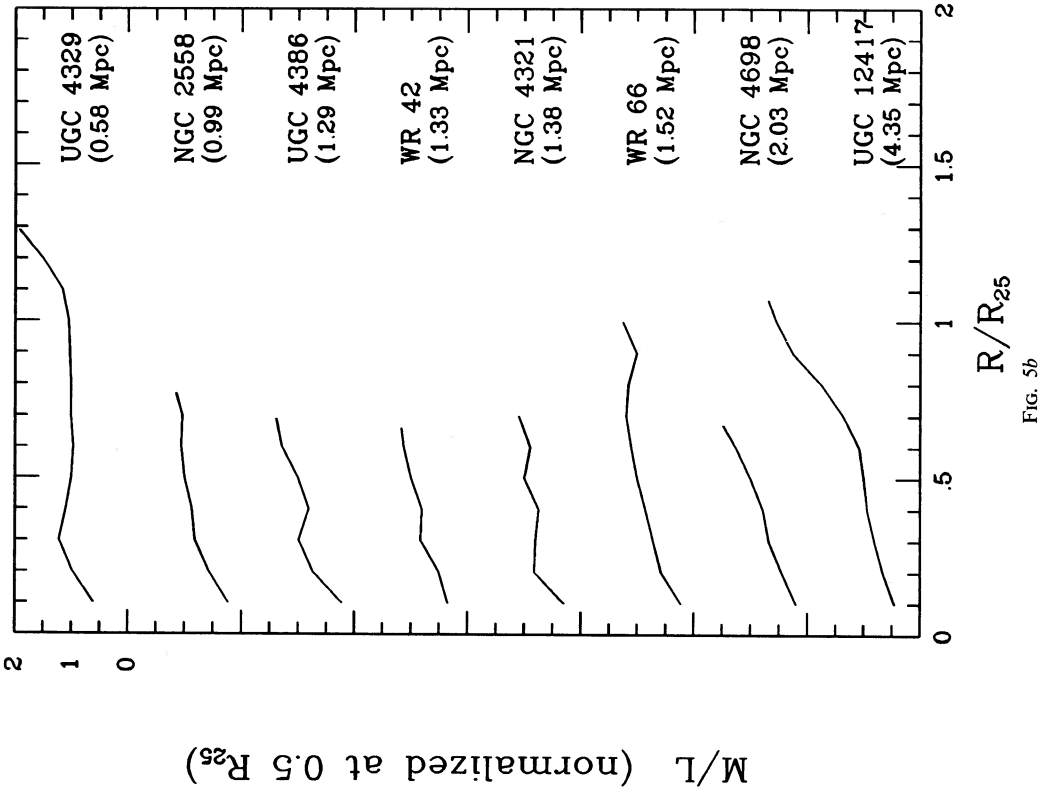

FIG. 5b

FIG. 5.—(*a*)–(*b*) Mass-to-light ratio (normalized to 1 at $0.5R_{25}$) vs. the distance from the center of the galaxy for the Hα cluster sample. Galaxies are arranged in order of the distance from the centers of the clusters, which are given in parentheses under the galaxy name. Note that the galaxies near the centers of clusters have flatter *M/L* gradients.

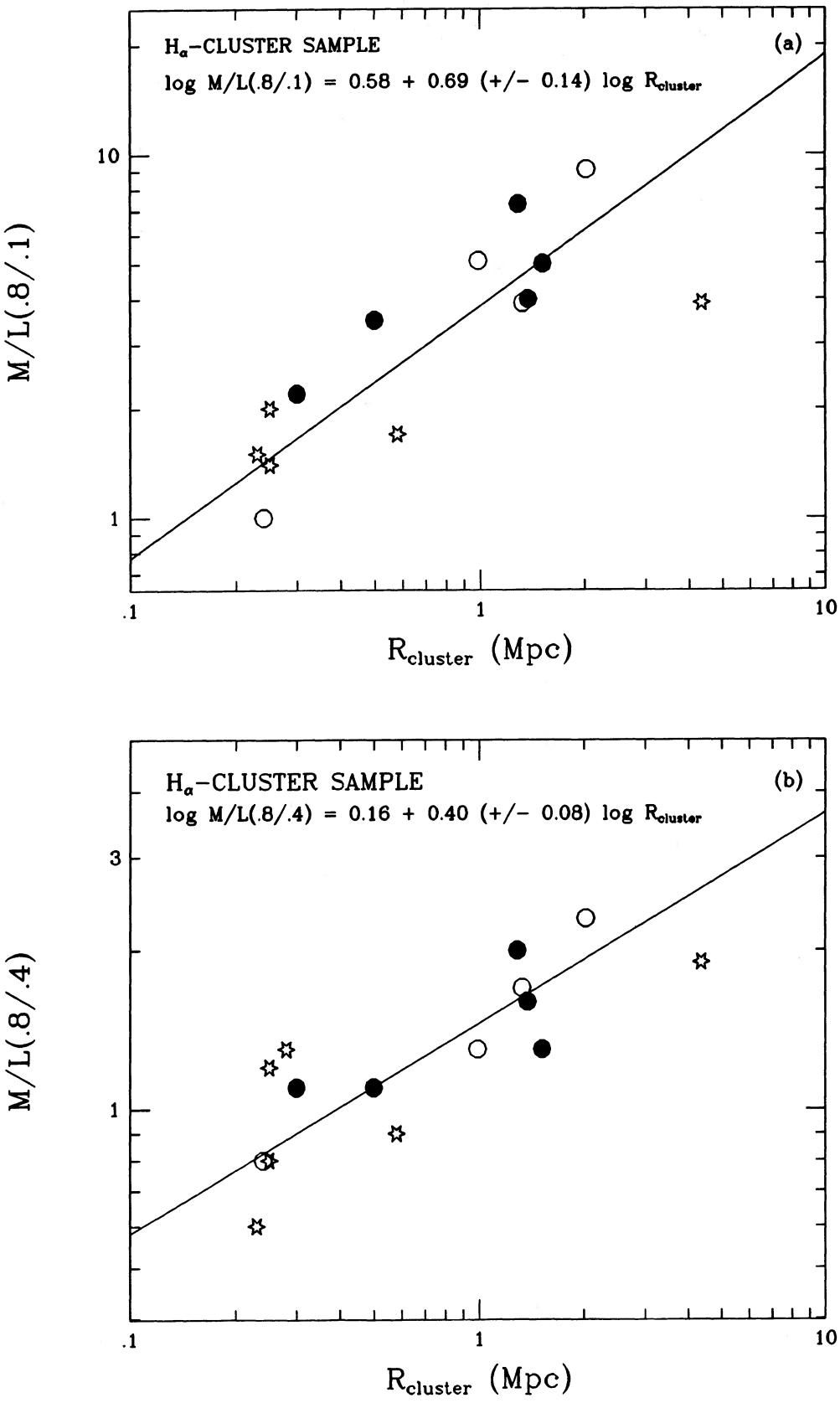

FIG. 6.—Mass-to-light ratio gradients vs. $R_{cluster}$ for the Hα cluster sample. (*a*) Gradient in M/L from $0.1R_{25}$ to $0.8R_{25}$. (*b*) Gradient in M/L from $0.4R_{25}$ to $0.8R_{25}$. Same symbol definition as Fig. 1. Steeper M/L gradients are found in galaxies in the outer regions of the clusters.

TABLE 2

PROPERTIES OF GALAXIES IN THE H I FIELD SAMPLE

Name (1)	Type (2)	M_B (mag) (3)	Distance (Mpc) (4)	R_{25} (kpc) (5)	R_f/R_{25} (6)	OG (%) (7)	EG (%) (8)	$\Delta V_{OBS-SYN}$ (km s^{-1}) (9)	V_{SLOPE} (10)
NGC 224	Sb	−21.91	0.67	26.1	1.15	−6	4	7	−53
NGC 247	Sc	−18.71	2.52	7.4	1.42	14	14	−7	−30
NGC 300	Sc	−18.34	1.90	6.1	1.39	22	1	−7	−6
NGC 2403	Sc	−19.75	3.25	10.0	1.94	10	5	14	−7
NGC 2841	Sb	−20.30	9.0	10.1	3.96	3	−6	131	33
NGC 2903	Sc	−20.24	6.1	11.6	2.02	−2	−1	81	−86
NGC 3031	Sb	−20.90	3.25	14.2	1.55	−18	−9	44	98
NGC 3109	SBm	−17.55	1.7	3.9	3.02	6	14	...	...
NGC 3198	Sc	−19.55	9.2	10.5	2.79	8	−2	43	−8
NGC 4236	SBd	−18.67	3.25	8.8	1.28	21	9	...	...
NGC 4258	Sb	−20.83	6.6	16.5	1.82	10	4	−1	−11
NGC 4736	Sab	−20.19	6.0	9.4	1.12	2	−24	5	−40
NGC 5033	Sbc	−20.64	14.0	20.4	1.76	3	3	51	16
NGC 5055	Sbc	−20.62	8.0	13.8	3.25	1	−6	58	−32
NGC 7331	Sb	−21.53	14.0	33.6	0.89	12	...	14	18
UGC 2259	Sc	−16.15	9.8	5.3	1.44	11	6	...	...

NOTES.—Key to columns is as follows:

Col. (2).—Hubble Type from Sandage and Tammann 1981 for the H I cluster sample, and from Kent 1987 (i.e., from RC2) for the H I field sample.

Col. (9).—The difference at $0.5R_{25}$ between the observed rotation curve and synthetic rotation curve using a fit within the range $0.4R_{25}$ and $0.8R_{25}$.

Col. (10).—Slope of the residuals between the observed rotation curve and synthetic rotation curves using a fit within the range $0.4R_{25}$ and $0.8R_{25}$.

Other columns same as Table 1.

previous sections on two samples of galaxies in order to compare results derived from Hα observations with results derived from H I observations. These are the following:

1. H I *field sample* (*16 galaxies*).—H I observations of field spirals with extended H I observations as compiled by Kent (1987).

2. H I *cluster sample* (*15 galaxies*).—H I observations of 15 of the 21 spirals in the Virgo cluster by Guhathakurta *et al.* (1988). The six galaxies which have been removed from the sample show effects of insufficient resolution (Guhathakurta *et al.* 1988).

i) *Velocity Gradients*

Tables 2 and 3 list the values of OG and EG for the H I field and H I cluster samples. Figure 7 shows the plot of the outer gradient (OG) versus $R_{cluster}$ for the H I cluster sample. Although we again find that the galaxies near the center of the cluster tend to have lower values of OG, the lack of many galaxies within 1 Mpc of the center of the Virgo cluster makes the correlation less prominent than for the Hα cluster sample. This gap is partially caused by the fact that the truncated H I disks near the center of the Virgo cluster do not extend far

TABLE 3

PROPERTIES OF GALAXIES IN THE H I CLUSTER SAMPLE[a]

Name (1)	Type (2)	M_B (mag) (3)	Distance (Mpc) (4)	R_{25} (kpc) (5)	R_f/R_{25} (6)	$R_{cluster}$ (Mpc) (7)	OG (%) (8)	EG (%) (9)	$\Delta V_{OBS-SYN}$ (km s^{-1}) (10)	V_{SLOPE} (11)	$M/L(0.8/0.4)$ (12)	H I Deficiency (13)
NGC 4178	SBc	−20.38	20.0	13.7	2.02	1.63	28	4	31	76	1.9	−0.13
NGC 4192	Sb	−22.12	20.0	30.9	1.37	1.70	19	−5	−37	141	1.8	0.09
NGC 4206	Sbc	−20.00	20.0	14.1	1.54	1.35	31	13	−58	54	2.6	−0.09
NGC 4216	Sb	−21.78	20.0	22.6	1.09	1.30	28	7	−30	197	2.1	0.35
NGC 4254	Sc	−21.75	20.0	18.6	1.33	1.25	15	14	3	21	1.8	0.02
NGC 4303	Sc	−21.42	20.0	17.6	1.73	2.87	3	1	−4	−36	1.3	0.17
NGC 4321	Sc	−21.67	20.0	20.9	1.18	1.38	12	−28	69	87	1.5	0.52
NGC 4388[b]	Sab	−21.18	20.0	15.7	0.65	0.44	2	...	−12	103	1.5	1.06
NGC 4402[b]	Sb	−20.42	20.0	12.8	0.57	0.47	...	...	...	...	...	0.61
NGC 4450	Sab(pec)	−20.84	20.0	13.6	0.96	1.65	12	...	9	35	1.6	1.31
NGC 4501	Sbc	−22.08	20.0	21.6	1.01	0.72	7	6	46	73	1.2	0.47
NGC 4535	SBc	−21.10	20.0	19.2	1.28	1.49	11	18	19	23	1.4	0.17
NGC 4548	SBb	−20.98	20.0	16.8	1.30	0.84	29	−4	30	134	1.9	0.86
NGC 4569[b]	Sab	−22.19	20.0	29.2	0.40	0.58	...	...	...	...	...	0.99
NGC 4579[b]	Sab	−21.63	20.0	18.5	0.63	0.62	−6	...	39	−54	1.1	1.01

[a] Same definitions as in previous tables.

[b] Beamwidth = 15″ for these galaxies; = 45″ for other galaxies in the H I cluster sample.

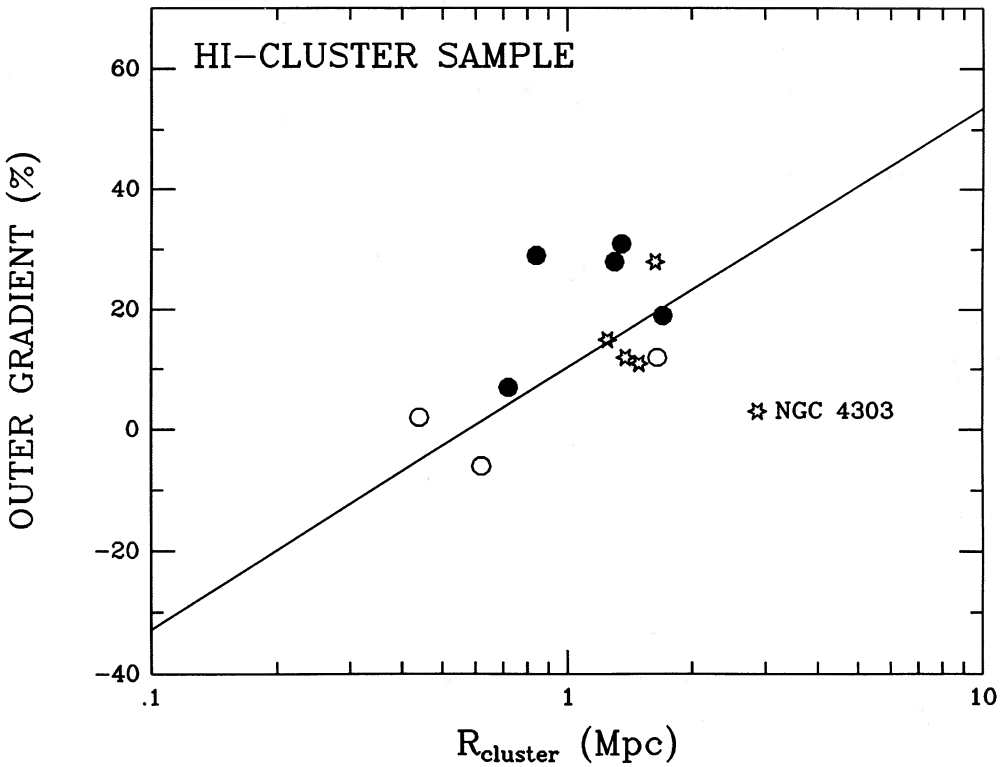

FIG. 7.—Outer gradient of the rotation curve vs. the projected distance from the center of the cluster for the H I cluster sample. Same symbol definitions as Fig. 1. The line is the best-fit line from the Hα cluster sample. NGC 4303, a member of the W cloud according to Binggeli *et al.* (1985), has a value $R_{cluster} = 0.52$ Mpc from the center of the cloud.

enough to determine OG (i.e., NGC 4402 and NGC 4569). The line in Figure 7 is the best-fit line for the Hα cluster sample from Figure 1.

It is interesting to note that according to Binggeli, Sandage, and Tammann (1985), the most discrepant galaxy, NGC 4303, is not a part of the main concentration of the Virgo cluster which is centered around M87, but is a member of the W cloud $\sim 7°$ south of M87. If NGC 4261 is used as the center of the W cloud, the projected distance for NGC 4303 would be $R_{cluster} = 0.52$ Mpc, placing it close to the line.

The poorer spatial resolution of the H I observations makes the use of the inner gradient (IG) of the rotation curves unprofitable. No clear correlation is seen between the extended gradient (EG) and $R_{cluster}$. However, nearly all of the galaxies with measured values of EG are in the outer regions of the cluster.

ii) *Comparison with Synthetic Rotation Curves*

A comparison between the rotation curves in the H I samples and synthetic rotation curves (Rubin *et al.* 1985) shows that within the inner $0.2R_{25}$ almost all of the observed rotation curves in the H I cluster are shallower than would be predicted by the synthetic rotation curves. This is clearly a result of the poorer resolution of the H I cluster sample (beamwidth = 45″ for most of the observations). The effect appears to reach to at least $0.4R_{25}$, making the comparison and the determinations of $\Delta V_{OBS-SYN}$ and V_{SLOPE} very uncertain. Nevertheless, if we limit our comparison to the region between $0.4R_{25}$ and $0.8R_{25}$, we again find that the inner cluster galaxies have flatter rotation curves than the outer cluster galaxies.

iii) *M/L Gradients*

Figure 8 shows the variation of integral M/L as a function of the distance from the center of the galaxy for the H I cluster sample. In the Hα sample, the inner cluster galaxies have flatter M/L gradients than the galaxies in the outer regions of the cluster. In the H I cluster sample this is only marginally discernible, presumably because of the lack of data for galaxies near the centers of clusters.

Values for the gradient in mass-to-light ratios from $0.4R_{25}$ to $0.8R_{25}$ are included in Table 3, and plotted in Figure 9 versus $R_{cluster}$. The superposed line is from the fit to the Hα cluster sample (Fig. 6) for comparison. The H I cluster sample shows the same trend as the Hα cluster sample, but the limited range in the values of $R_{cluster}$ make the correlation less pronounced. NGC 4303 is again the most deviant point.

f) Correlations with H I *Deficiency*

Figures 10 and 11 show the relation between the H I deficiency (Giovanelli and Haynes 1985) and $R_{cluster}$ for the Hα cluster and H I cluster samples. The fact that the inner cluster galaxies tend to be deficient in H I has been well established by a number of studies (see Haynes, Giovanelli, and Chincarini 1984 for a review). While the trend is clearly seen in both our cluster samples, the H I deficiency versus $R_{cluster}$ does not appear to be as well defined as the OG or M/L gradients versus $R_{cluster}$ correlations.

Figures 12 and 13 show the relation between H I deficiency and the outer gradient of the rotation curve for the Hα cluster and H I cluster samples. The lack of a well-defined relation between these two parameters suggests that the same physical mechanism may not be responsible for producing both the H I

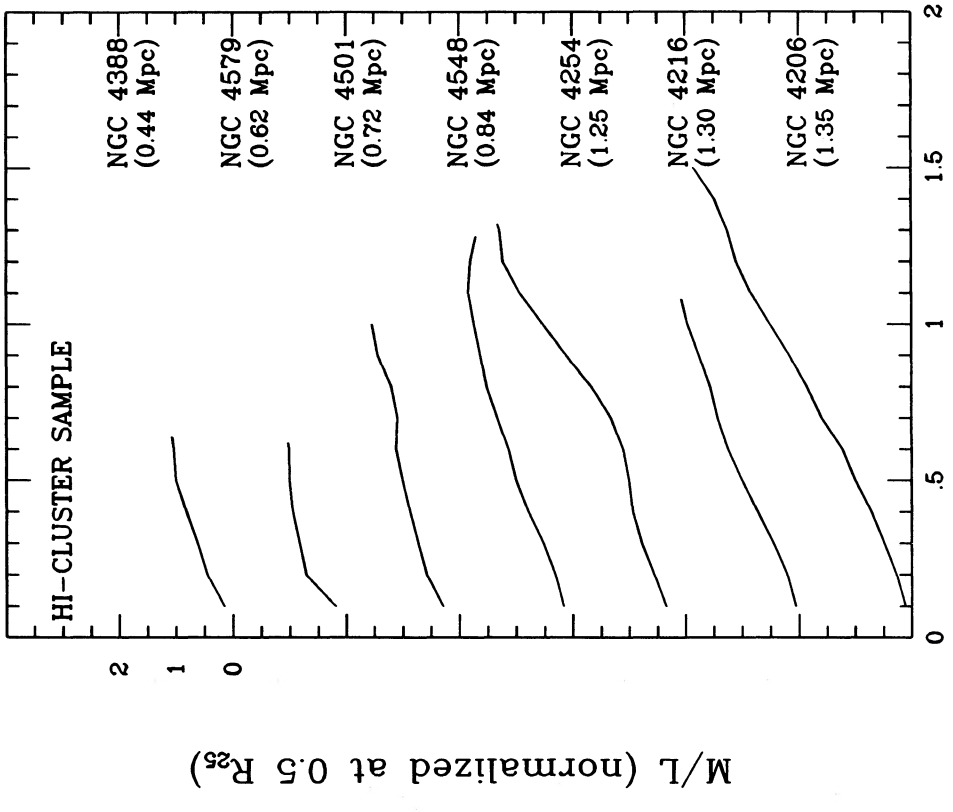

FIG. 8a

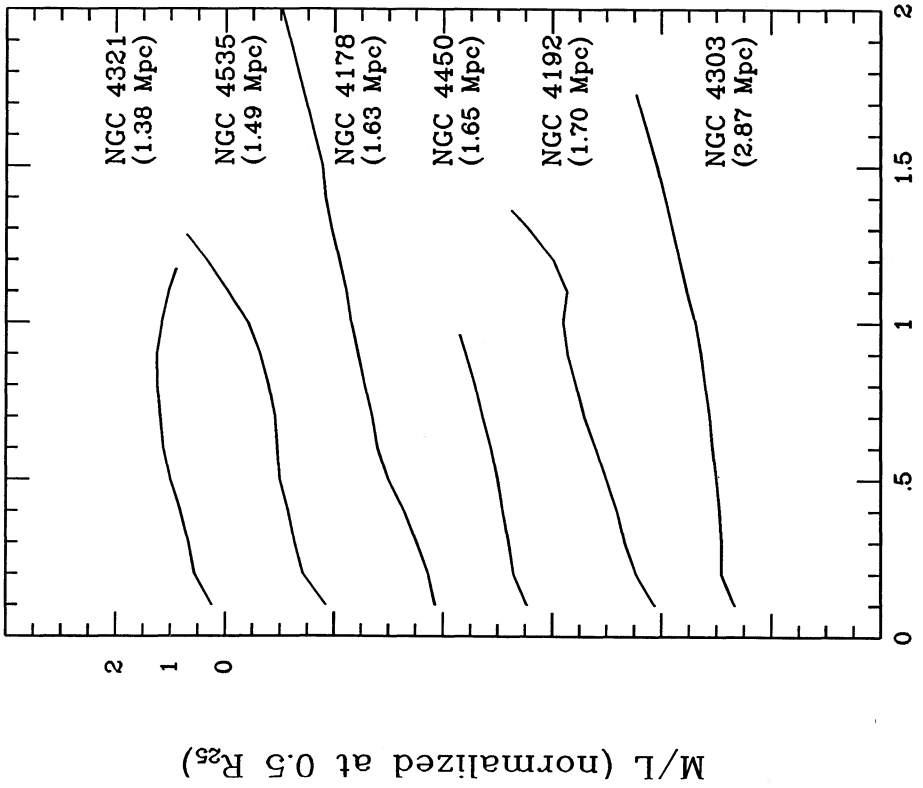

FIG. 8b

FIG. 8.—(*a*)–(*b*) Mass-to-light ratio (normalized to 1 at $0.5R_{25}$) vs. the distance from the center of the galaxy for the H I cluster sample. The galaxies are arranged in order of the distance from the center of the cluster, which is given in parentheses under the galaxy name.

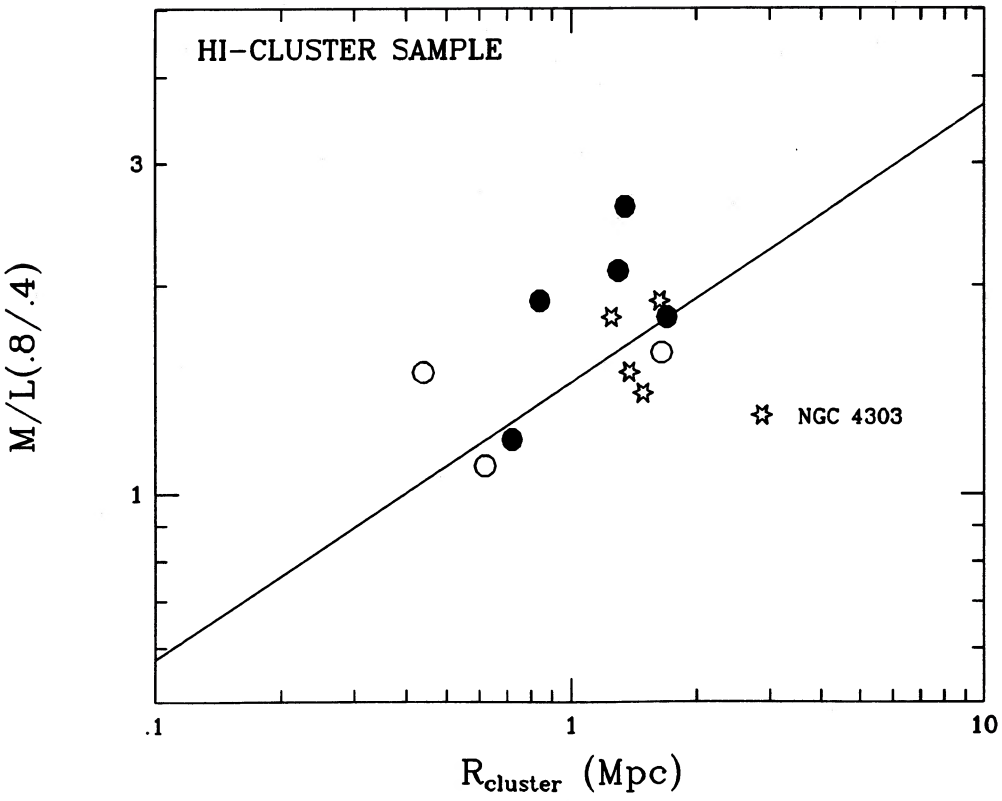

FIG. 9.—Mass-to-light gradient from $0.4R_{25}$ to $0.8R_{25}$ vs. $R_{\rm cluster}$ for the H I cluster sample. The superposed line is the best-fit from the Hα cluster sample (Fig. 6). Same symbol definition as Fig. 1.

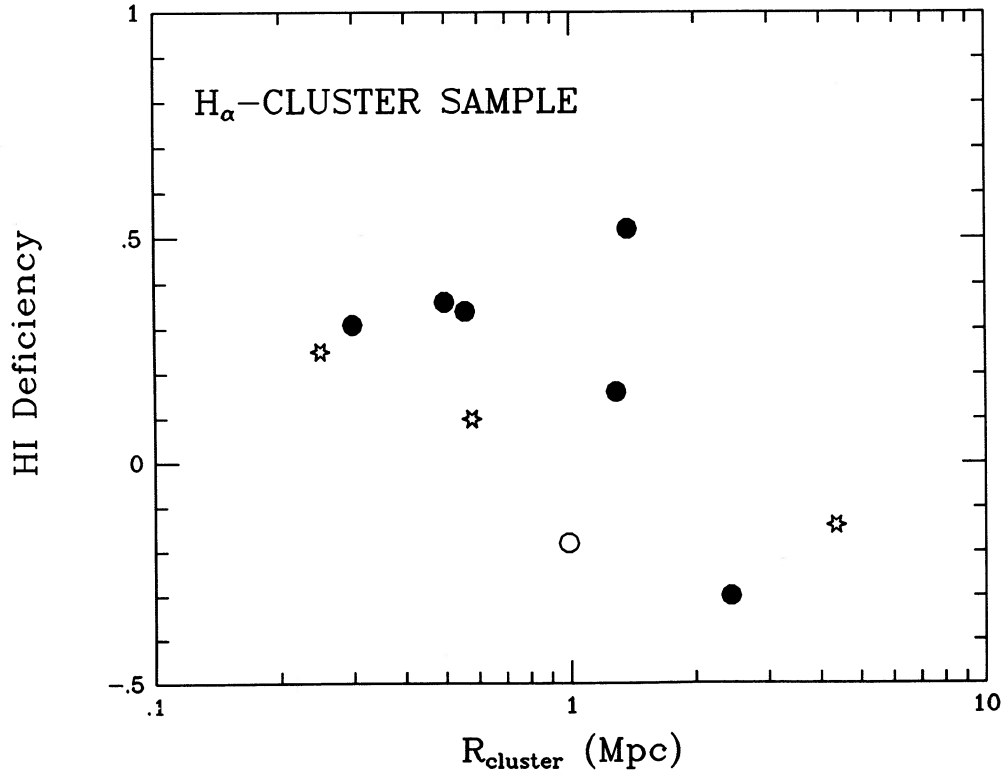

FIG. 10.—H I deficiency from Giovanelli and Haynes (1985) vs. projected distance from the center of the cluster for the Hα cluster sample. The inner galaxies are more deficient in neutral hydrogen, as previously found for larger samples (Haynes, Giovanelli, and Chincarini 1984).

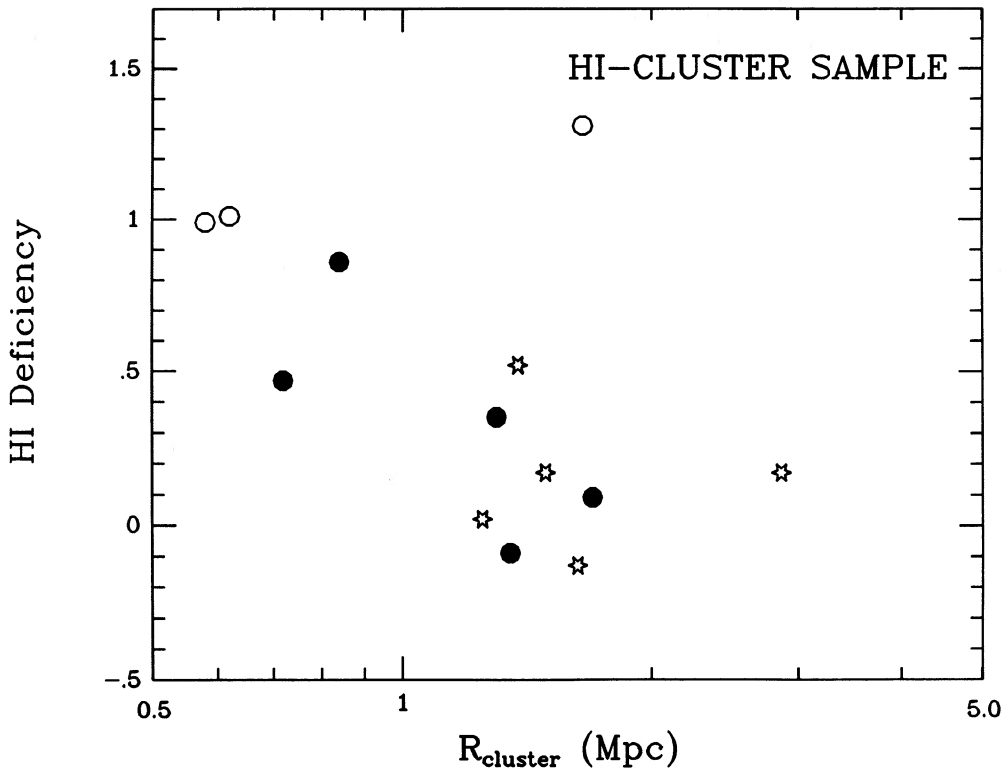

FIG. 11.—H I deficiency vs. projected distance from the center of the cluster for the H I cluster sample. A weak trend is found for the inner galaxies to be more deficient in neutral hydrogen.

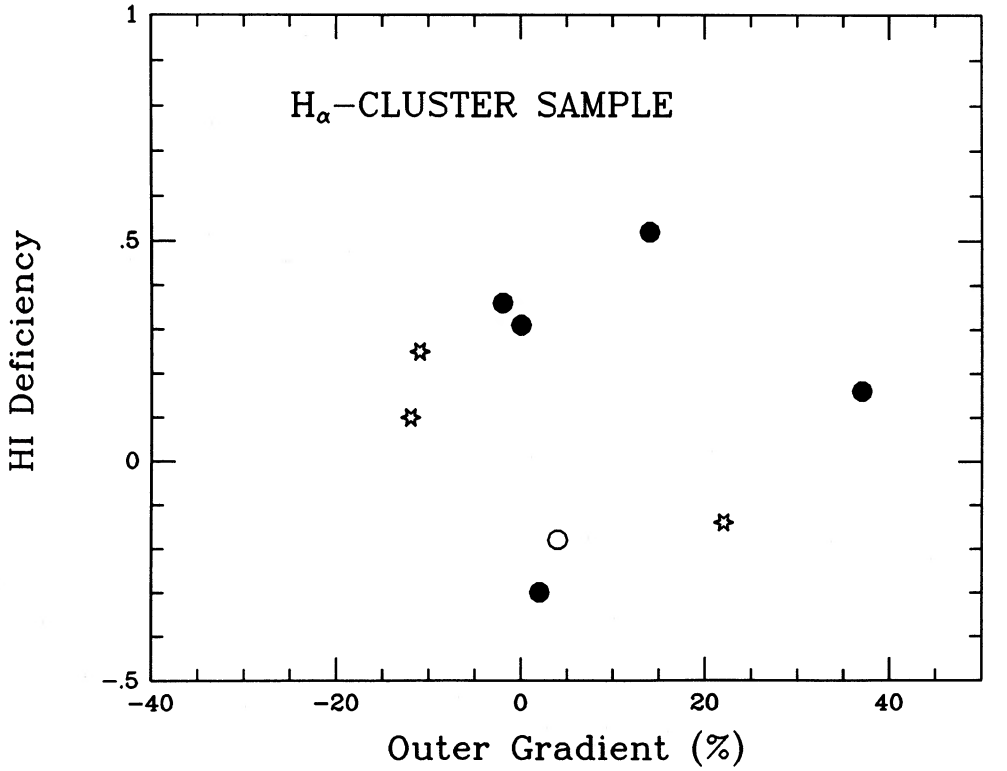

FIG. 12.—H I deficiency vs. the outer gradient of the rotation curve for the Hα cluster sample. The lack of a strong correlation suggests different physical mechanisms are responsible for the deficiency of neutral hydrogen and the falling rotation curves.

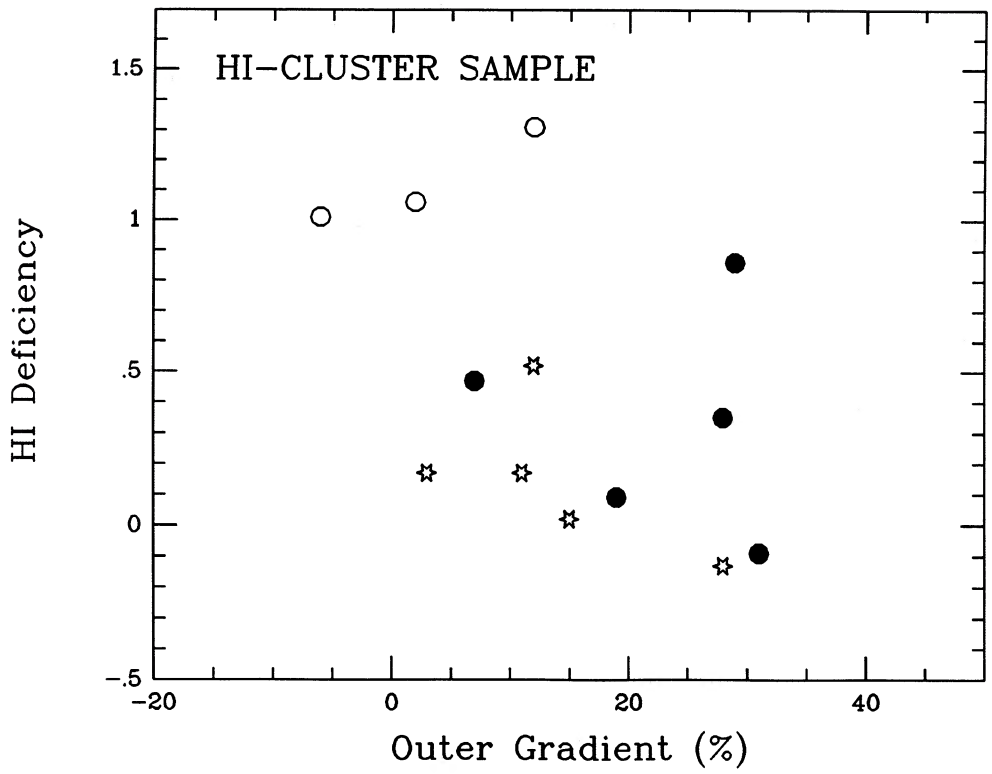

FIG. 13.—H I deficiency vs. the outer gradient of the rotation curve for the H I cluster sample

deficiencies and the falling rotation curves for spiral galaxies in the inner regions of clusters.

III. SUMMARY

Based principally on Hα emission-line rotation curves, we find that the properties of cluster galaxies vary as a function of distance from the centers of clusters. Galaxies located in the inner regions have falling rotation curves and integral M/L ratios which increase slowly with galaxy radius; galaxies located in the outer regions have flat or rising rotation curves and integral M/L values which increase more rapidly. The most likely interpretation is that dynamical interactions in the higher density regions of the clusters have modified the outer material of the spiral galaxies.

The study used the following criteria:

1. Velocity gradients:

For the Hα cluster sample, a good correlation is found between the outer velocity gradient from $0.4R_{25}$ to $0.8R_{25}$ with the distance from the center of the clusters. The H I cluster sample supports the correlation but is not as well defined, presumably because it has few galaxies near the center of the cluster.

The galaxies in the outer regions of the clusters tend to have shallower inner gradients (measured at $0.15R_{25}$) than their counterparts near the center of the cluster, or in the field. The statistical significance of this result is only marginal.

2. Residuals from synthetic rotation curves:

The residuals between the Hα cluster observations and the Rubin *et al.* (1985) synthetic rotation curves for field galaxies show the same trend as found in the outer gradient; galaxies near the centers of clusters tend to have falling rotation curves compared to the outer cluster galaxies or to the field galaxies. The H I cluster sample shows the same trend, but the poorer spatial resolution for the H I observations makes the result more uncertain.

3. M/L gradients:

A strong correlation is found between the gradient in the mass-to-light ratio (from $0.1R_{25}$ to $0.8R_{25}$ and from $0.4R_{25}$ to $0.8R_{25}$) and the position in the cluster. The galaxies with steeper M/L gradients, and, presumably, larger fractions of dark matter, tend to be found in the outer regions of clusters. The H I cluster sample supports the correlation, but the lack of extended velocity information for galaxies near the cluster center again makes the correlation less obvious.

Clusters of galaxies, even loose clusters like Cancer, Hercules (A2151), and Peg I, contain spiral galaxies near their centers whose properties differ from those in the outer cluster, and in the field. Although some optical properties for cluster spirals appear to be indistinguishable from field spirals (Kennicut, Bothun, and Schommer 1984), and the CO disks appear normal (Kenney and Young 1986), spirals near the cluster center are likely to be H I deficient (Haynes, Giovanelli, and Chincarini 1984; Dressler 1986), and to have truncated and asymmetric H I disks (Warmels 1985). We now add two additional physical properties which appear to be modified for spiral galaxies in the inner regions of clusters: these galaxies appear to have falling rotation curves, and their M/L gradients are flatter than for galaxies in the outer regions of clusters.

We would like to thank Steve Kent for supplying his mass model programs and P. Guhathakurta, J. van Gorkom, C. Kotanyi, and C. Balkowski for allowing us to use their data prior to publication. We would also like to thank Steve Kent, Jacqueline Van Gorkom, and Bill Oegerle for reading the manuscript and offering useful comments.

TABLE 4

LUMINOSITY PROFILES IN *R* FOR GALAXIES IN THE CANCER AND HERCULES CLUSTERS

RADIUS (ARCSEC)	CANCER CLUSTER						FOREGROUND		HERCULES CLUSTER			
	NGC 2558		UGC 4329		UGC 4386		UGC 4375		NGC 6045		NGC 6054	
	MAJ.	MIN.	MAJ.	MIN.	MAJ.	MIN.	MAJ.	MIN.	MAJ.	MIN.	MAJ.	MIN.
0.00	17.71	17.71	19.20	19.20	17.80	17.80	18.44	18.44	18.25	18.25	18.86	18.86
0.87	17.87	17.87	19.50	19.47	18.03	18.11	18.66	18.67	18.43	18.47	19.17	19.20
1.75	18.04	18.10	19.99	19.91	18.30	18.73	18.96	18.99	18.71	18.88	19.66	19.82
2.62	18.37	18.63	20.46	20.38	18.67	19.46	19.26	19.35	19.02	19.47	20.17	20.43
3.49	18.84	19.27	20.66	20.62	18.89	19.92	19.47	19.61	19.31	20.11	20.53	20.95
4.37	19.15	19.74	20.75	20.61	19.12	20.31	19.60	19.78	19.59	20.83	20.83	21.46
5.24	19.45	20.20	20.83	20.51	19.34	20.75	19.70	20.00	19.70	21.34	21.04	21.94
6.11	19.71	20.58	20.91	20.70	19.57	21.06	19.80	20.16	19.80	21.79	21.30	22.26
6.99	19.97	20.85	20.99	20.91	19.72	21.34	19.88	20.26	19.92	22.22	21.63	22.44
7.86	20.16	21.03	21.10	21.13	19.83	21.56	19.95	20.34	20.09	22.66	21.93	22.47
8.73	20.35	21.18	21.23	21.23	19.92	21.75	20.03	20.46	20.21	23.10	22.22	22.50
9.61	20.58	21.33	21.43	21.20	20.01	22.01	20.08	20.66	20.29	23.41	22.50	22.87
10.48	20.73	21.45	21.58	21.19	20.02	22.25	20.21	20.59	20.39	23.57	22.72	23.14
11.35	20.89	21.56	21.64	21.22	19.98	22.22	20.27	20.60	20.53	23.89	22.92	23.15
12.23	21.01	21.65	21.68	21.32	19.98	22.55	20.27	20.61	20.70	24.24	23.05	23.48
13.10	21.11	21.73	21.69	21.37	20.16	22.70	20.29	20.80	20.77	...	23.31	23.84
13.97	21.22	21.76	21.71	21.39	20.34	22.88	20.32	20.87	20.84	...	23.29	24.43
14.85	21.31	21.77	21.81	21.69	20.47	23.04	20.39	21.08	20.89	...	23.30	...
15.72	21.38	21.79	21.92	21.88	20.56	23.30	20.46	21.15	20.99	...	23.70	...
16.59	21.46	21.84	22.00	22.01	20.60	23.48	20.62	21.27	21.12	...	23.26	...
17.90	21.55	21.93	22.09	22.16	20.66	23.71	20.71	21.11	21.16	...	23.34	...
19.65	21.59	22.09	22.26	22.37	20.70	24.14	20.84	21.38	21.22	...	23.44	...
21.40	21.58	22.26	22.47	22.62	20.70	24.09	20.93	21.64	21.29	...	23.42	...
23.15	21.63	22.48	22.71	22.87	20.72	23.98	20.96	21.87	21.45	...	23.50	...
24.89	21.77	22.71	22.87	23.03	20.72	24.35	21.02	22.22	21.60	...	23.79	...
26.64	21.93	22.96	22.93	23.08	20.76	...	21.19	22.35	21.75	...	...	...
28.39	22.13	23.17	23.03	23.31	20.93	...	21.38	22.29	21.91	...	...	...
30.13	22.28	23.21	23.20	23.50	21.11	...	21.54	21.78	22.54	...	...	...
31.88	22.38	23.39	23.29	23.53	21.13	...	21.57	22.04	22.74	...	...	...
33.63	22.36	23.51	23.61	23.66	21.01	...	21.77	22.29	23.20	...	...	...
35.81	22.69	23.74	23.71	23.88	21.00	...	21.70	22.62	23.54	...	...	...
38.43	22.77	23.94	23.59	24.34	21.40	...	21.86	22.75	...	...	...	...
41.05	23.00	24.29	23.60	...	21.70	...	22.18	22.94	...	...	...	...
43.67	23.19	24.48	23.95	...	21.99	...	22.07	22.90	...	...	...	...
46.29	23.41	...	23.83	...	22.14	...	22.40	23.33	...	...	...	...
48.91	23.72	...	...	...	22.34	...	22.60	24.00	...	...	...	...
51.53	23.82	...	23.75	...	22.56	...	22.79	...	...	...	...	...
55.02	24.22	...	24.34	...	22.95	...	23.09	...	...	...	...	...
59.39	...	...	...	...	23.42	...	23.07	...	...	...	...	...
63.76	...	...	...	...	24.09	...	...	...	...	...	...	...
68.13	...	...	...	...	24.33	...	23.70	...	...	...	...	...
72.49	...	...	...	...	...	...	...	...	...	...	...	...
76.86	...	...	...	...	...	...	23.98	...	...	...	...	...

APPENDIX

RED PHOTOMETRY OF CLUSTER AND FIELD GALAXIES

Observations of Cancer and Hercules galaxies were made by Rubin using the KPNO No. 1 36″ telescope with the TI-3 CCD detector in 1987 March. The Mould *R*-band filter was used with an effective wavelength of ~6500 Å. The reductions were essentially identical to those reported in Whitmore, McElroy, and Schweizer (1987). Apparent *R* magnitudes for the major and minor axis profiles are listed in Table 4. Figure 14 shows the major and minor axis luminosity profiles for the galaxies in the Cancer and Hercules clusters. Figure 15 shows the major and minor axis luminosity profiles for four galaxies from the Hα field sample used to check the accuracy of our reductions. Apparent *R* magnitudes for these four galaxies are listed in Table 5.

TABLE 5

LUMINOSITY PROFILES IN *R* FOR REFERENCE GALAXIES

RADIUS (ARCSEC)	NGC 2715		NGC 2742		NGC 2998		NGC 3593	
	MAJ.	MIN.	MAJ.	MIN.	MAJ.	MIN.	MAJ.	MIN.
0.00	18.95	18.95	18.98	18.98	18.43	18.43	16.96	16.96
0.87	19.02	19.04	19.01	19.04	18.65	18.72	17.09	17.04
1.75	19.16	19.24	19.15	19.24	19.01	19.25	17.32	17.44
2.62	19.39	19.55	19.33	19.50	19.28	19.54	17.45	17.89
3.49	19.58	19.75	19.53	19.78	19.52	19.78	17.56	18.09
4.37	19.76	19.95	19.68	19.99	19.65	19.95	17.68	18.21
5.24	19.90	20.12	19.82	20.12	19.73	20.19	17.77	18.45
6.11	20.02	20.20	19.94	20.21	19.75	20.27	17.80	18.80
6.99	20.13	20.26	20.01	20.29	19.82	20.33	17.81	19.23
7.86	20.23	20.32	20.13	20.37	19.91	20.28	17.93	19.55
8.73	20.30	20.36	20.19	20.46	19.99	20.34	18.14	19.67
9.61	20.35	20.43	20.23	20.49	20.02	20.61	18.39	19.81
10.48	20.38	20.50	20.26	20.50	20.01	21.07	18.64	19.93
11.35	20.40	20.51	20.28	20.52	20.04	21.32	18.77	19.98
12.23	20.43	20.54	20.33	20.55	20.15	21.52	18.82	20.04
13.10	20.46	20.57	20.36	20.59	20.41	21.62	18.87	20.05
13.97	20.50	20.55	20.38	20.63	20.63	21.62	18.90	20.19
14.85	20.52	20.58	20.42	20.68	20.91	21.61	18.87	20.24
15.72	20.52	20.61	20.45	20.75	21.05	21.58	18.90	20.34
16.59	20.52	20.65	20.48	20.81	21.13	21.63	19.11	20.47
17.90	20.54	20.74	20.48	20.90	21.17	21.80	19.31	20.54
19.65	20.58	20.87	20.48	21.05	21.01	22.12	19.23	20.72
21.40	20.54	21.02	20.48	21.22	20.87	22.51	19.36	20.84
23.15	20.54	21.16	20.52	21.32	20.90	22.96	19.53	21.03
24.89	20.51	21.27	20.58	21.35	21.02	23.16	19.66	21.22
26.64	20.47	21.45	20.60	21.39	21.05	23.21	19.75	21.40
28.39	20.39	21.69	20.65	21.45	21.17	23.15	19.93	21.45
30.13	20.29	21.96	20.66	21.54	21.57	23.16	20.06	21.65
31.88	20.30	22.16	20.66	21.67	21.95	23.48	20.15	21.76
33.63	20.52	22.41	20.68	21.86	22.15	23.81	20.23	21.94
35.81	20.83	22.70	20.78	22.19	22.25	23.79	20.26	22.00
38.43	21.08	22.95	20.90	22.58	22.22	23.90	20.25	22.25
41.05	21.25	23.26	20.96	22.97	22.14	...	20.36	22.46
43.67	21.40	23.57	21.11	23.19	22.26	...	20.50	22.68
46.29	21.60	23.89	21.35	23.54	22.40	...	20.53	22.79
48.91	21.75	24.20	21.48	23.68	22.63	...	20.65	...
51.53	21.83	24.42	21.58	24.00	22.77	...	20.79	22.97
55.02	21.86	...	21.69	24.20	23.40	...	21.01	23.02
59.39	21.80	...	21.60	24.47	23.86	...	21.20	23.20
63.76	21.92	...	21.56	...	23.62	...	21.32	23.57
68.13	22.07	...	21.78	...	23.54	...	21.41	23.91
72.49	22.17	...	21.98	...	23.44	...	21.43	23.94
76.86	22.25	...	22.44	...	24.19	...	21.59	...
81.23	22.41	...	22.86	...	...	...	21.67	...
85.59	22.41	...	23.27	...	...	...	21.76	...
92.14	22.48	...	23.77	...	...	...	21.88	...
100.88	22.62	...	24.27	...	...	...	22.15	...

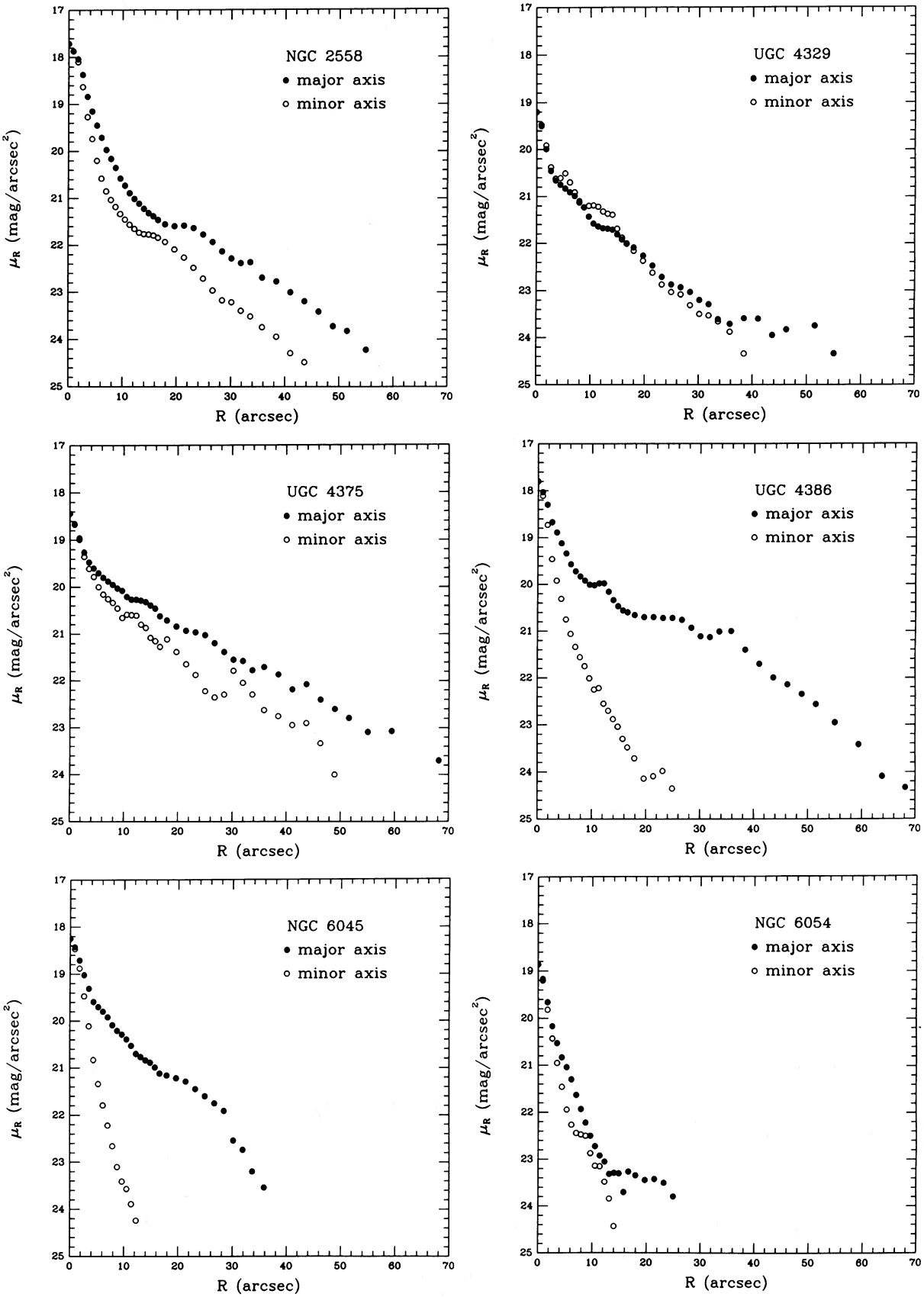

FIG. 14.—Major and minor luminosity profiles in the Mould *R* band for the galaxies in the Cancer and Hercules clusters

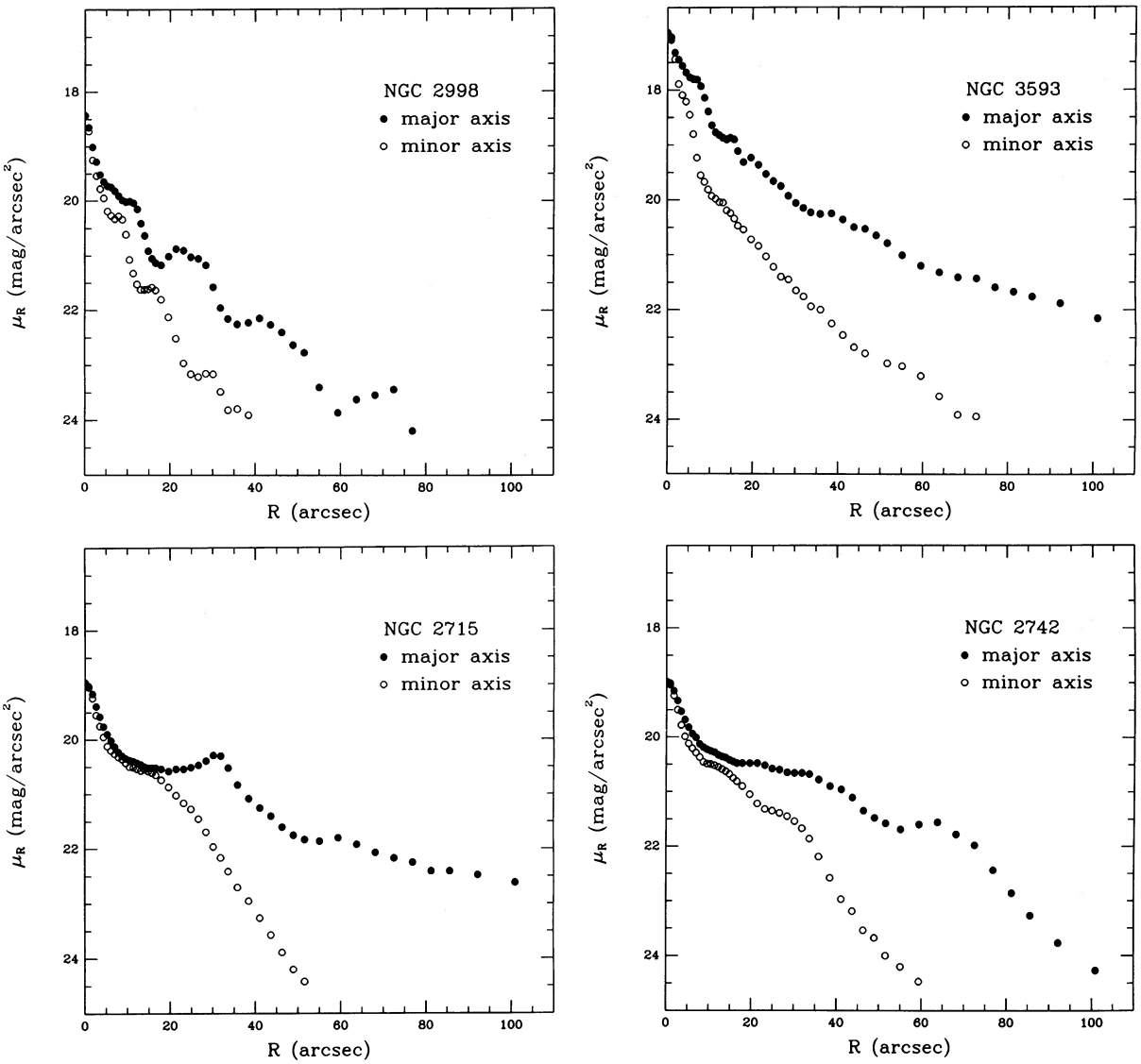

FIG. 15.—Major and minor luminosity profiles in the Mould *R* band for four field galaxies

REFERENCES

Athanassoula, S., Bosma, A., and Papaioannou, S. 1987, *Astr. Astr.*, **179**, 23.
Bell, M., and Whitmore, B. C. 1988, in preparation.
Binggeli, B., Sandage, A., and Tammann, G. A. 1985, *A.J.*, **90**, 1681.
Burstein, D., Rubin, V. C., Ford, W. K., and Whitmore, B. C. 1986, *Ap. J. (Letters)*, **305**, L11.
Chincarini, G., and de Souza, R. 1985, *Astr. Ap.*, **153**, 218.
de Vaucouleurs, G., de Vaucouleurs, A., and Corwin, H. G. 1976, *Second Reference Catalogue of Bright Galaxies* (Austin: University of Texas Press) (RC2).
Dressler, A. 1980, *Ap. J.*, **236**, 351.
———. 1984, *Ann. Rev. Astr. Ap.*, **22**, 185.
———. 1986, *Ap. J.*, **301**, 35.
Forbes, D. A., and Whitmore, B. C. 1988, in preparation.
Giovanelli, R., and Haynes, M. 1985, *Ap. J.*, **292**, 404.
Guhathakurta, P., van Gorkom, J. H., Kotanyi, C. G., and Balkowski, C. 1988, preprint.
Haynes, M. P., Giovanelli, R., and Chincarini, G. L. 1984, *Ann. Rev. Astr. Ap.*, **22**, 445.
Hubble, E., and Humason, M. L. 1931, *Ap. J.*, **74**, 43.
Kalnajs, A. J. 1983, in *IAU Symposium 100, Internal Kinematics and Dynamics of Galaxies*, ed. E. Athanassoula (Dordrecht: Reidel), p. 87.
Kenney, J. D., and Young, J. 1986, *Ap. J. (Letters)*, **301**, L13.
Kent, S. 1986, *A.J.*, **91**, 1301.
———. 1987, *A.J.*, **93**, 816.
———. 1988, preprint.
Kennicutt, R. C., Bothun, G. D., and Schommer, R. A. 1984, *A.J.*, **89**, 1279.
Rubin, V. C. 1983, in *IAU Symposium 100, Internal Kinematics and Dynamics of Galaxies*, ed. E. Athanassoula (Dordrecht: Reidel), p. 3.
Rubin, V. C., Burstein, D., Ford, W. K., Jr., and Thonnard, N. 1985, *Ap. J.*, **289**, 81.
Rubin, V. C., Whitmore, B. C., and Ford, W. K., Jr. 1988, *Ap. J.*, **333**, 522 (Paper I).
Sandage, A., and Tammann, G. A. 1981, *A Revised Shapley-Ames Catalog of Bright Galaxies* (Washington, DC: Carnegie Institution of Washington) (RSA).
Warmels, R. H. 1985, in *The Virgo Cluster*, ed. O-G. Richter and B. Binggeli (Garching: ESO), p. 51.
Whitmore, B. C. 1984, *Ap. J.*, **278**, 61.
Whitmore, B. C., McElroy, D., and Schweizer, F. 1987, *Ap. J.*, **314**, 439.

DUNCAN A. FORBES and BRADLEY C. WHITMORE: Space Telescope Science Institute, 3700 San Martin Drive, Baltimore, MD 21218

VERA C. RUBIN: Department of Terrestrial Magnetism, Carnegie Institution of Washington, 5241 Broad Branch Rd., N.W., Washington, DC 20015